Human Molecular Genetics, 2005, Vol. 14, No. 21 ***3219–3225***
doi:10.1093/hmg/ddi352
Advance Access published on October 3, 2005

ZNF217 suppresses cell death associated with chemotherapy and telomere dysfunction

Guiqing Huang[1], Sheryl Krig[3], David Kowbel[1], Hongmei Xu[1], Bill Hyun[1], Stas Volik[1], Burt Feuerstein[2], Gordon B. Mills[4], David Stokoe[1], Paul Yaswen[3] and Colin Collins[1,*]

[1]Cancer Research Institute and [2]Brain Tumor Research Center of the Department of Neurological Surgery, The University of California San Francisco, San Francisco, CA 94143-0808, USA, [3]Life Sciences Division, Lawrence Berkeley National Laboratory, Berkeley, CA 94720, USA and [4]Department of Molecular Therapeutics, University of Texas MD, Anderson Cancer Center, Houston, TX, USA

Received July 24, 2005; Revised and Accepted September 16, 2005

Chromosome 20q13.2 is amplified in 20–30% of early-stage breast tumors and is associated with poor prognosis. Detailed mapping of the amplified region using molecular cytogenetics, positional cloning and genomic sequencing culminated in a detailed molecular description of the candidate oncogene *ZNF217*. *ZNF217* proteins resemble Kruppel-like transcription factors, localize predominately to the nucleus and associate with proteins involved in transcriptional repression. The findings that *ZNF217* can immortalize human mammary epithelial cells and that its amplification is associated with poor prognosis suggest that it may play roles in both early- and late-stage breast cancer. We present evidence that *ZNF217* can attenuate apoptotic signals resulting from telomere dysfunction as well as from doxorubicin-induced DNA damage and that silencing *ZNF217* with siRNA restores sensitivity to doxorubicin. Moreover, elevated *ZNF217* leads to increased phosphorylation of Akt, whereas inhibition of the phosphatidylinositol 3 kinase pathway and Akt phosphorylation decreases *ZNF217* protein levels and increases sensitivity to doxorubicin. These results suggest that *ZNF217* may promote neoplastic transformation by increasing cell survival during telomeric crisis and may promote later stages of malignancy by increasing cell survival during chemotherapy.

INTRODUCTION

DNA amplification at chromosome position 20q13 is common in human breast tumors (1), appears to be an early event (2), correlates with poor prognosis (3) and may reflect the presence of at least two important, previously uncharacterized oncogenes (4). Amplification of 20q13 was initially discovered in 40% of breast cancer cell lines and 18% of primary breast tumors, using comparative genomic hybridization (CGH) (1). In a study of 132 primary breast carcinomas and 11 metastases, 20q13.2 amplification was found in 29% of the cases (3). Amplification was associated with high histologic grade, aneuploidy and high S-phase fraction. High-level amplification was associated with short, disease-free survival of patients with node negative breast cancer. Independent studies employing CGH have identified 20q13 amplification in colon, bladder, ovarian and brain cancers (5–9), suggesting this amplification may contribute to tumor progression in a wide spectrum of the most common cancers.

To identify the oncogene(s) driving amplification of 20q13.2, we pursued a positional cloning and genomic sequencing strategy that resulted in the identification of seven genes: *ZNF217*, *ZNF218*, *NABC3*, *NABC2*, *NABC1*, *CYP24* and *PIC-like* (10). Of these genes, only *ZNF217* and *NABC1* were expressed in breast cancer cell lines amplified at the 20q13.2 locus and only *ZNF217* mapped within the 260 kb minimum common amplicon defined in over 300 tumors and cell lines (10). We have shown that *ZNF217* is expressed at levels that correlate with the degree of amplification in specific cell lines and tumors (10). Thus, *ZNF217* emerged as a strong candidate for the oncogene driving 20q13.2 amplification.

Full-length *ZNF217* cDNAs encode two open-reading frames of 1062 and 1108 amino acids, because of alternative splicing of exon 4. Each predicted protein has eight C2H2 zinc fingers and a proline-rich domain. Sequence analysis of *ZNF217* indicates a strong resemblance to members of the Kruppel-like family of zinc finger proteins (11). Other members of the Kruppel-like family have been implicated in

*To whom correspondence should be addressed. Tel: +1 4155027065; Fax: +1 4154768218; Email: collins@cc.ucsf.edu

several human malignancies, including WT1 in Wilms tumor and GLI1 in glioblastoma. The eight zinc finger domains in *ZNF217* are interspersed throughout the *ZNF217* sequence, and their pattern does not appear to fall into one of the three classes: triple-C2H2, multiple-adjacent-C2H2 and separated-paired-C2H2 finger proteins (reviewed in 12). The sixth and seventh zinc fingers in *ZNF217* are separated by the conserved linker sequence, TGEKP, reported to bind DNA with high affinity (13). Database analysis indicates that this paired zinc finger region aligns with those in several members of the Delta-EF1/ZFH-1 family of two-handed zinc-finger homeodomain proteins, including Smad-interacting protein 1 (14).

As members of the Kruppel family are involved in many aspects of growth, differentiation and development, the precise function of *ZNF217* and its possible role in tumorigenesis could not be predicted on the basis of homology alone. *ZNF217* protein localizes to the nucleus (4) and co-immunoprecipitates with complexes containing the transcriptional corepressors CoREST and CtBP, histone deacetylases HDAC1 and 2 and histone methyltransferases G9a and Eu-HMTase1 (15,16). This strongly suggests that *ZNF217* may function as part of a transcriptional repressor complex. Changes in CtBP expression, in turn, can modulate the cellular threshold for apoptotic responses by contributing to the repression of certain proapoptotic genes (17). These include well-established p53 target genes as well as genes that are not known to be regulated by p53. Although CtBP does not appear to be a direct antagonist of transactivation by p53, there is a significant overlap in target genes inversely regulated by the two factors.

Additional clues to a possible *ZNF217* function come from a cell culture study that found that human uroepithelial cells immortalized after exposure to the HPV16 E7 oncogene routinely contained extra chromosome 20q material (18). This work suggested that *ZNF217* or another gene within the amplified region might complement E7's role in immortalization. In addition, the average number of additional chromosome 20 signals increased with passage in one such E7 expressing line, suggesting that the amplification might confer a selective advantage in culture. An association between high-level 20q13.2 amplification and genome instability was also reported, despite the presence of wild-type p53, suggesting that 20q gain might generate or enable cells to tolerate increased genome instability.

RESULTS

To investigate the cellular consequences of *ZNF217* overexpression in tumor cells, we transfected HeLa cells with a plasmid encoding a *ZNF217*–enhanced green fluorescent protein (EGFP) fusion. Control HeLa cells express low levels of endogenous *ZNF217* (data not shown). Cells accumulated faster in *ZNF*217–EGFP transfected cultures than in either parallel control cultures of non-transfected cells or cells transfected with an EGFP construct alone (Fig. 1A). In three independent experiments, ~40% more EGFP positive cells were present in *ZNF217*–EGFP transfected cultures when compared with control EGFP cultures 72 h after plating equal numbers of cells. Analysis of DNA content showed no apparent difference in cell-cycle distribution between the two populations of cells (data not shown). However, the proportion of floating cells accumulating propidium iodide (PI), an indicator of loss of viability, was significantly lower in *ZNF217*–EGFP transfected cultures than that in either non-transfected cells or cells transfected with an EGFP construct alone (Fig. 1B). Assays of Annexin-V staining, an independent indicator of cell death, confirmed that spontaneous cell death was suppressed in HeLa cells expressing *ZNF217*–EGFP (data not shown).

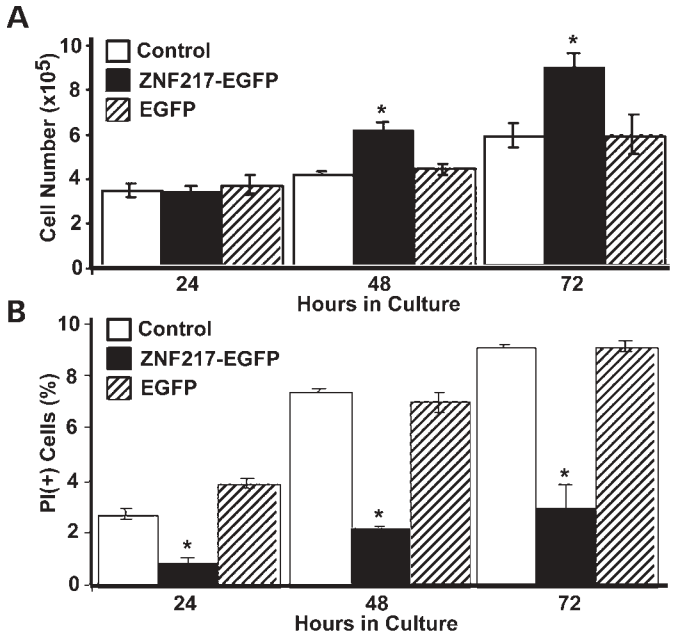

Figure 1. Cells accumulate faster in *ZNF217*–EGFP-transfected HeLa cell cultures and undergo a lower rate of spontaneous cell death than that in parallel control cultures. (**A**) Non-transfected (white), *ZNF217*–EGFP transfected (black) or EGFP vector transfected (striped) cells were plated in triplicate in six-well plates and grown in medium. At 24, 48 and 72 h after plating, cells were harvested and counted. (**B**) At indicated times, adherent and non-adherent cells were combined, stained with PI and analyzed by flow cytometry. The percentage of PI(+) cells corresponds to the percentage of dead cells in the respective cultures. Each experimental point represents the mean of at least three independent experiments ± standard deviation. An asterisk denotes $P \leq 0.005$ for those cultures transfected with *ZNF217*–EGFP when compared with EGFP alone.

To determine whether *ZNF217* prevented cell death induced by different mechanisms, we assayed the responses of cells expressing different levels of either endogenous or exogenously introduced *ZNF217* to doxorubicin. Doxorubicin is a chemotherapeutic agent known to inhibit topoisomerase II and to induce double-strand DNA breaks, resulting in ATM/p53-mediated apoptosis (19). The HBL100 cell line, which expresses relatively low levels of endogenous *ZNF217* transcripts, was found to be much more sensitive to doxorubicin-induced cell death than either the MCF7 or the 600MPE (Fig. 2A), both of which express high levels of endogenous *ZNF217* transcripts (10). To directly assess the protective effect of *ZNF217* against doxorubicin-induced cell death, we compared HeLa and HBL100 cells transfected with *ZNF217*–EGFP with control cells. In multiple independent experiments in both cell types, *ZNF217*–EGFP-expressing cells displayed statistically significant lower levels of

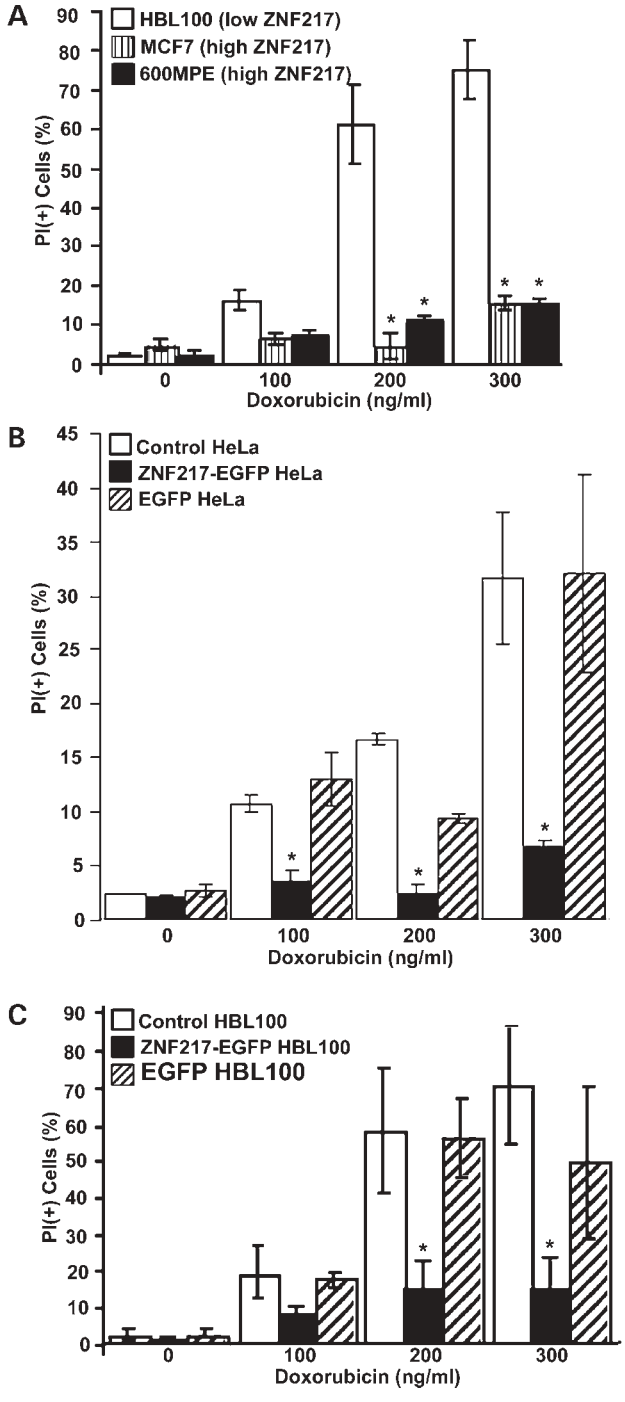

Figure 2. Cells expressing high levels of endogenous *ZNF217* transcripts or exogenously introduced *ZNF217* genes are resistant to doxorubicin-induced cell death. In (**A**–**C**), the cells were exposed to the indicated concentrations of doxorubicin for 72 h. The percentage of dead (PI^+) cells in each culture was then measured by flow cytometry. (A) HBL100 (white) shows no amplification and low expression of *ZNF217*, whereas MCF7 (striped) shows amplification and high expression of *ZNF217* and 600MPE (black) shows no amplification, but high expression of *ZNF217* (10). (B and C) Control non-transfected (white), *ZNF217*–EGFP transfected (black) and EGFP vector transfected (striped) HeLa (B) and HBL100 (C) cells were analyzed for sensitivity to doxorubicin. In (A), asterisk denotes $P \leq 0.005$ when compared with HBL100. In (B and C), asterisk denotes $P \leq 0.005$ for those cultures transfected with *ZNF217*–EGFP when compared with EGFP alone. Representative primary flow cytometry data for (C) is provided as Supplementary Material.

doxorubicin-induced cell death than non-transfected or EGFP-transfected controls (Figs 2B and C).

To establish whether *ZNF217* plays a direct role in conferring resistance to doxorubicin, four siRNA molecules were selected to specifically down-modulate its expression in the MCF7 cells. SiRNAs 1, 2 and 3 all elicited increased cell killing by doxorubicin, and siRNAs 1 and 2 were shown to knock down *ZNF*217 mRNA and/or protein (mRNA and protein levels were not evaluated for siRNA 3). Transfection of siRNA 4 into MCF7 had no effect on *ZNF*217 mRNA or protein level or cell death (data not shown). Maximum knockdown of both *ZNF*217 mRNA and protein was achieved with siRNA 1, which was used for further studies. Transient transfection with this *ZNF217*-targeted siRNA resulted in reduction of both *ZNF217* mRNA and protein levels when compared with control cells transfected with scrambled control RNA in HBL100, HBL100 transfected with *ZNF217*–EGFP (Z-HBL100), BT474, MCF7 and three brain tumor cell lines with low (SF188), medium (U251) and high (U251 + 7.9) relative expression of *ZNF217* (data not shown) (Fig. 3A). In three independent experiments, transfection with *ZNF217* siRNA 1 resulted in an increase in spontaneous cell death and cell death induced by doxorubicin (Fig. 3B). The data are consistent with the hypothesis that in the cells in which it is highly expressed, *ZNF217* supports basic cell survival as well as survival in response to DNA damage.

The ability of *ZNF217* to confer resistance to spontaneous and doxorubicin-induced cell death in multiple transformed cell lines suggests that its expression may be selected for whenever cell survival is threatened during multiple stages of tumor progression. Our past work (20) showed that expression of exogenously introduced *ZNF217* does not directly activate telomerase expression in human mammary epithelial cells, but that it allows a subset of such cells to continue growing when control cells have succumbed to growth arrest and cell death associated with critically short telomeres. We hypothesized that high *ZNF217* expression protects against telomere dysfunction-induced growth arrest and/or cell death. To test this hypothesis directly, we manipulated the levels and function of telomere binding proteins, TRF1 and TRF2, to disrupt telomere integrity in cell lines expressing different levels of endogenous or exogenous *ZNF217*. Expression of a dominant negative TRF2 mutant ($TRF2^{\Delta B\Delta M}$) has previously been shown to trigger ATM/p53 dependent apoptosis (21), whereas over-expression of wild-type TRF1 has been shown to cause ATM/p53 independent cell death in susceptible cells (22). Transiently transfected $TRF2^{\Delta B\Delta M}$ or TRF1 induced significantly less cell death in the MCF7 and 600MPE, which express endogenous *ZNF217* at high levels, than that induced in HBL100 or HeLa cells, which express low levels of endogenous *ZNF217* (Fig. 4). In HBL100 and HeLa cells transfected with both $TRF2^{\Delta B\Delta M}$ and *ZNF217*–EGFP, the level of cell death was 3–5-fold lower than that observed in cells transfected with $TRF2^{\Delta B\Delta M}$ alone. Similarly, transient transfection with TRF1 alone induced significant cell death in HeLa and HBL100 cells, whereas cotransfection with *ZNF217*–EGFP attenuated cell death in the same cell lines.

Akt activation is known to promote cellular survival in a variety of experimental systems. Activated Akt directly

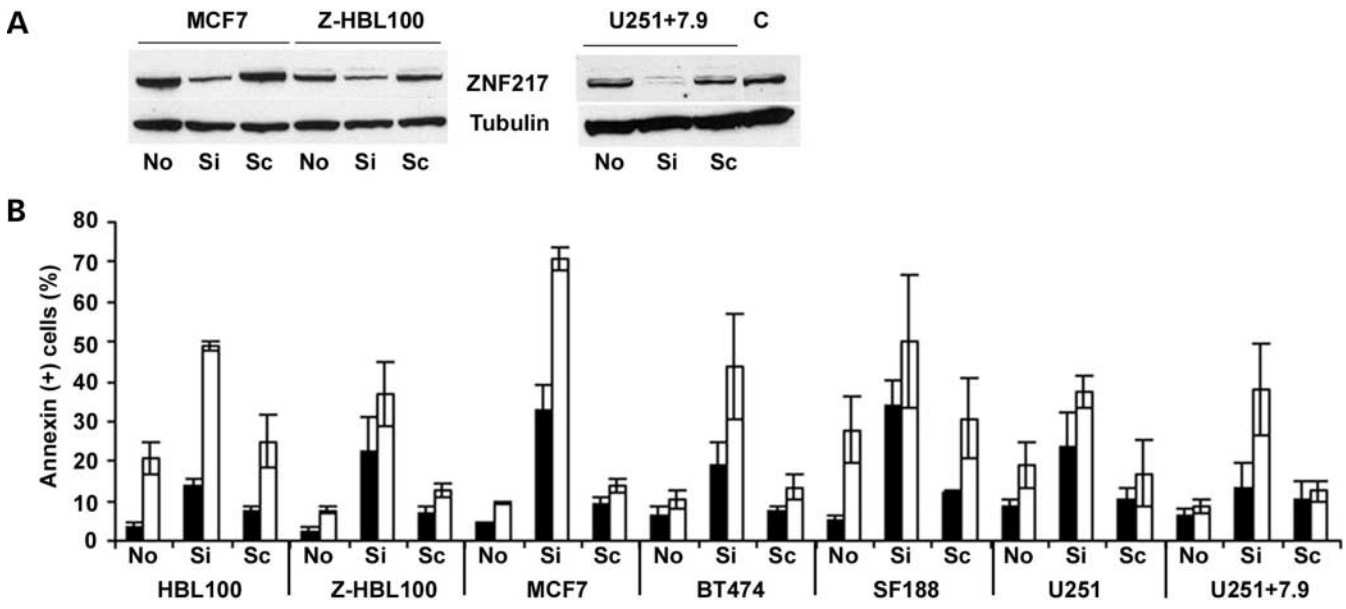

Figure 3. *ZNF217*-targeted siRNA down-modulates *ZNF217* protein levels and enhances cell killing by doxorubicin. (**A**) Levels of *ZNF217* or tubulin protein were compared by immunoblotting of total cell lysates of human cell lines MCF7, *ZNF217*–EGFP-transfected HBL100 (Z-HBL100) and U251 + 7.9 non-transfected (No), transfected with siRNA directed against *ZNF217* transcripts (Si) or transfected with a control scrambled siRNA (Sc) for 72 h. C is a control lysate containing high levels of *ZNF217* protein expressed from a retroviral promoter. *ZNF217* protein was quantitated in total cell lysates by immunoblot analysis using an anti-*ZNF217* antibody raised against a synthetic peptide. (**B**) The percentages of dead or dying cells staining positively with Annexin-V were plotted for the indicated cell lines non-transfected (No), transfected with siRNA directed against *ZNF217* transcripts (Si) or transfected with a control scrambled dsRNA (Sc) for 72 h, then treated with 0 (black) or 100 ng/ml (white) doxorubicin for 16 h before harvest.

phosphorylates key mediators of the apoptotic cascade and indirectly regulates the expression of pro- and anti-apoptotic genes (23,24). To begin to elucidate the mechanism by which *ZNF217* promotes cell survival, we asked whether increased cellular *ZNF217* protein leads to activation of the phosphatidylinositol 3′ kinase (PI3K) pathway, as indicated by elevated levels of phosphorylated Akt. Transfection of HBL100 with *ZNF217*–EGFP resulted in increased phosphorylation of Akt (Ser-473) relative to the non-transfected HBL100 cells that weakly express *ZNF217* (Fig. 5). In the MCF7 cell line in which *ZNF217* is amplified, we detected high levels of both *ZNF217* protein and phosphorylated Akt (Ser-473), without a concomitant increase in total AKT levels, relative to HBL100 cells. Silencing *ZNF217* with siRNA resulted in decreased Akt (Ser-473) phosphorylation. Finally, inhibition of PI3K and thus Akt phosphorylation with the PI3K inhibitor Ly294002 reduced both Akt phosphorylation and *ZNF217* protein levels in the MCF7, and this was accompanied by increased apoptosis in response to doxorubicin (data not shown). In all cases, the levels of total Akt were relatively unchanged. The data are therefore consistent with the concepts that *ZNF217* effects on cell survival are mediated at least partly through activation of the PI3K/AKT pathway, and that there is a feedback regulation between the Akt pathway and *ZNF217* expression.

DISCUSSION

We have found that *ZNF217* can attenuate apoptotic signals emanating from DNA damage by a common therapeutic agent and from functionally compromised telomeres. This finding is highly significant because it may explain how elevated *ZNF217* expression contributes to both early and late stages of tumor progression. *ZNF217* may act early to promote survival of preneoplastic cells with dysfunctional telomeres and later to confer resistance to chemotherapy. Absence of adequate TTAGGG repeat DNA or artificially disrupted binding of telomeric proteins may cause telomeric DNA to resemble double-stranded breaks, which are the predominant initiating signals for ATM-mediated p53 activation (22). Doxorubicin also causes double-stranded DNA breaks by inhibition of topoisomerase II. Therefore, the growth arrest and cell death caused by these two disparate stimuli may share common elements mediated by p53 activation. However, the ability of *ZNF217* to protect against TRF1 induced cell killing suggests that *ZNF217* can also attenuate an ATM/p53 independent pathway.

The mechanism by which *ZNF217* expression promotes cell survival may involve phosphorylation of Akt, as high levels of endogenous *ZNF217* were correlated with high levels of phosphorylated Akt. Moreover, artificially increasing *ZNF217* protein levels increased Akt phosphorylation, whereas siRNA-mediated *ZNF217* silencing resulted in decreased phosphorylation of Akt. Furthermore, there may also be a feedback between PI3K activity and *ZNF217* expression. Upstream inhibition of Akt phosphorylation by blocking PI3K with Ly294002 reduced both phosphorylated Akt and *ZNF217* protein in the MCF7 cell line, resulting in increased apoptosis in response to doxorubicin. The positive feedback loop between *ZNF217* and the PI3K pathway could provide a self-reinforcing amplification of the effect of increased *ZNF217* DNA copy number.

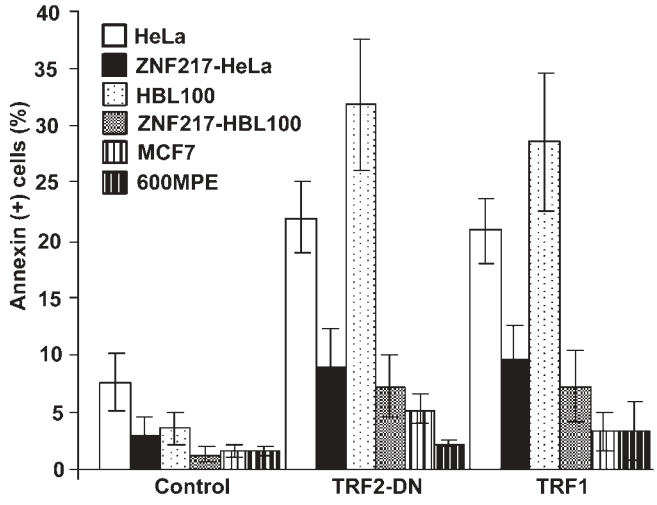

Figure 4. *ZNF217* expression protects cells from cell death induced by functional inactivation of TRF2 or by over-expression of TRF1. Cells were transfected with plasmids encoding TRF1 or TRF2$^{\Delta B\Delta M}$, and after 24 h, the transfection reagent was removed. Apoptosis assays were performed 48 h later. The percentages of apoptotic (Annexin-V^{+}) HeLa (white), *ZNF217*–EGFP transfected HeLa (black), HBL100 (light speckled), *ZNF217*–EGFP transfected HBL100 (dark speckled), MCF7 (light striped) and 600MPE (dark striped) cells were measured by flow cytometry. Note that both MCF7 and 600MPE contain high levels of endogenous *ZNF217* and are relatively resistant to cell death.

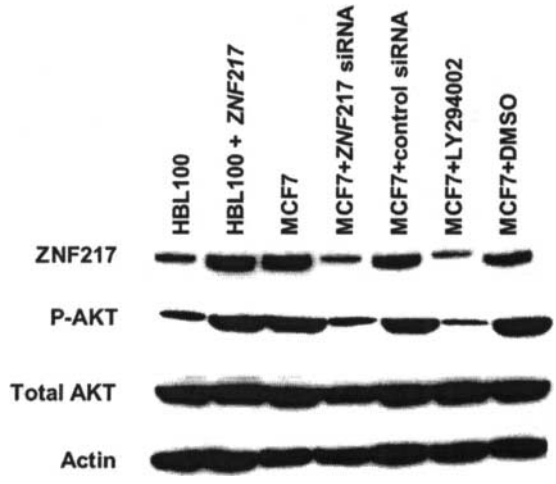

Figure 5. *ZNF217* expression causes elevated Akt phosphorylation, whereas silencing of *ZNF*217 causes a reduction of Akt phosphorylation and the inhibition of PI3K causes a reduction in *ZNF217* levels. Levels of *ZNF217*, phosphorylated Akt (Ser-473), total Akt or β-actin proteins were compared by immunoblotting of total cell lysates of human cell lines HBL100, *ZNF217*–EGFP transfected HBL100, MCF7, *ZNF*217 siRNA transfected MCF7, control siRNA transfected MCF7, PI3K inhibitor LY294002 treated MCF7 and DMSO vehicle treated MCF7.

ZNF217 protein localizes to the nucleus (4) and co-immunoprecipitates with complexes containing the transcriptional corepressors CoREST and CtBP, histone deacetylases HDAC1 and 2 and histone methyltransferases G9a and Eu-HMTase1 (15,16). This suggests that *ZNF217* may function as part of a transcriptional repressor complex and that aberrant transcriptional repression and recruitment of corepressors are mechanisms involved in *ZNF217*-induced cancer associated phenotypes. The hypothesized target genes through which *ZNF217* expression suppresses apoptosis have yet to be elucidated. The observation that *ZNF217* may regulate phosphorylated Akt suggests that *ZNF217*-regulated genes lie upstream of this important apoptosis regulator.

The current findings may have important clinical ramifications. We present data which demonstrate that aberrant *ZNF217* expression promotes both survival and proliferation of cells *in vitro* by a mechanism that may occur both early in the neoplastic process when telomeres become limiting and then at a later stage by conferring resistance to double-strand breaks induced by chemotherapy. This hypothesis could explain why patients with tumors having amplification of 20q13.2 have such a poor prognosis (3,25). In addition, we provide evidence that the anti-apoptotic activity of *ZNF217* may be mediated through activation of the PI3K pathway and Akt. Aberrant expression of *ZNF217* may occur even in cells with normal *ZNF217* gene copy number (4,10), possibly making cells less responsive to apoptotic signals. It will be important to determine the degree to which *ZNF217* expression levels vary in human populations and whether there is a correlation between the level of expression and either a susceptibility to cancer or its clinical outcome. Our findings support a model that unifies clinical, genomic and cell biological data. Most importantly, our data suggest that abrogation of *ZNF217* function in tumors with elevated *ZNF217* protein levels may render these tumors more sensitive to existing anti-tumor therapies.

MATERIALS AND METHODS

Cells and cell culture

The HeLa, HBL100, MCF7, BT474 and U251 cell lines were obtained from American Type Culture Collection (ATCC) and cultured as suggested by the supplier. The 600MPE cell line was obtained and cultured as previously described (10). The SF188 cell line was obtained from the tissue bank at the Brain Tumor Research Center at the University of California, San Francisco. The U251 + 7.9 clone was produced by transferring normal human chromosome 7 into the U251 cell line (unpublished data).

Transfections

Full-length *ZNF217* cDNAs in the plasmid pEGFP-N1 (Clontech, Palo Alto, CA, USA) or pEGFP-N1 alone were transfected into cells using Fugene 6 (Roche, Indianapolis, IN, USA), according to the manufacturers' protocol. EGFP positive populations were sorted by flow cytometry and replated into medium containing 500 μg/ml Geneticin (G418; Gibco BRL) for continued culture. Experiments were performed with stably transfected cells in which the EGFP^{+} percentage was greater than 80. For transient transfections of dominant negative TRF2 mutant (TRF2$^{\Delta B\Delta M}$) (21) and TRF1 (22), cells were plated at a density of 1.5×10^{5} cells per well in six-well plates. On day 2 following plating, the cells were transfected with plasmids encoding TRF1 or

TRF2$^{\Delta B\Delta M}$, and after 24 h, the transfection reagent was removed. Apoptosis assays were performed 48 h later.

Measurement of cell death

At indicated times, adherent cells were harvested by trypsinization and combined with non-adherent cells in culture medium. After centrifugation, the cells were resuspended in phosphate buffered saline and filtered (70 μm nylon mesh) to remove aggregates. PI was added to a final concentration of 50 μg/ml before analysis by flow cytometry (FACSCalibur, Becton Dickinson, San Jose, CA, USA). Triplicate samples were assayed to determine percentage of live (PI^-) versus dead (PI^+) cells. For p*ZNF217*–EGFP-N1 and pEGFP-N1 transfected cells, 30 000 events were first gated to exclude small debris, then analyzed for percentage of live (GFP^+ PI^-) versus dead GFP^+ (GFP^+ PI^+) cells.

Apoptosis assay

Adherent and non-adherent cells were collected, washed twice with phosphate buffered saline, then resuspended in 100 μl of binding buffer (10 mM HEPES, 140 mM NaCl and 2.5 mM $CaCl_2$, pH 7.4). Annexin-V antibody of 7.5 μl (Molecular Probes, Eugene, OR, USA) was added and the cells were incubated at room temperature for 15 min. After incubation, 400 μl of binding buffer was added and cell samples were analyzed by flow cytometry. For p*ZNF217*–EGFP-N1 and pEGFP-N1 transfected cells, the events were gated to measure percentage of GFP^+ Annexin-V^- versus GFP^+ Annexin-V^+ cells.

Gene silencing

Commercial software (Qiagen; Valencia, CA, USA) was used to design four candidate siRNA molecules mapping outside *ZNF217* zinc finger motifs and lacking detectable sequence similarity to other genes. The 19-nucleotide RNAs targeting *ZNF217* corresponded to regions beginning 591- (1: 5′-CGA UCAACGAGGUCGUCCA-3′), 722- (2: 5′-ACUGCUUU CGGUACCAGCA-3′), 970- (3: 5′-CGACGAUUCGAGUU CCGAG-3′) and 2830-bp (4: 5′-GUACCAUAUGGUCAGA GGC-3′) downstream of the first nucleotide of the start codon. Synthesis, purification and pre-annealing of siRNAs were performed by the vendor. SiRNA was transfected into cell lines with Oligofectamine (Invitrogen, Carlsbad, CA, USA), according to the manufacturer's protocol. Maximal down-modulation of *ZNF217* mRNA and protein was achieved with siRNA 1, and this siRNA was used for further studies. A scrambled duplex RNA (5′-AGUAUGGAUGGGGAGGCA C-3′) designed using Oligoengine software (Oligoengine, Seattle, WA, USA) and a commercial negative control siRNA (Qiagene Catalog no. 1022076, ACGUGACACGUUCGGA GAA) were used as negative controls. Control siRNA showed neither any silencing of *ZNF217* gene expression nor effect on doxorubicin-mediated apoptosis (data not shown).

PI3K inhibition

Growing cultures of MCF7 were treated with 10 μM of the PI3K inhibitor Ly294002 (Calbiochem, La Jolla, CA, USA) for 24 h, after which cells were harvested for immunoblot analysis. For assays of cell death, cells were treated with the Ly294002, followed 4 h later by the addition of 100 ng/ml doxorubicin. After an additional 16 h, the apoptotic cells were stained with Annexin-V antibody and analyzed by flow cytometry, as described earlier.

Immunoblot analysis

Total cell lysates were made with lysis buffer (20 mM Tris–HCL, pH 7.5, 150 mM NaCl, 25 mM NaF, 1 mM EDTA, 1 mM EGTA, 1 mM DTT, 1 mM $NaVO_4$, 0.5% NP-40, 0.2%SDS and 1× Protease Inhibitor Cocktail Set III (Calbiochem, La Jolla, CA, USA). Protein concentrations were determined. Twenty microgram aliquots were mixed with SDS–PAGE sample buffer and separated by gel electrophoresis. Proteins were transferred onto blotting grade PVDF membranes (Osmonics Inc., Minnetonka, MN, USA) using an XCell II Blot Module (Invitrogen, Carlsbad, CA, USA). *ZNF217*, pAkt, total Akt and β-actin protein levels were detected by immunoblot analysis using a polyclonal antibody developed against a *ZNF217*–GST fusion peptide, a monoclonal antibody against phosphorylated Akt (Ser-473) (26), a polyclonal antibody against total Akt (Cat. no. SC-8312; Santa Cruz Biotechnology, Santa Cruz, CA, USA) and a monoclonal antibody against β-actin (Cat. no. A1978; Sigma, Saint Louis, MO, USA).

Statistical analysis

The significance of differences observed was calculated using Student's *t*-test. Values were judged to be significant when $P \leq 0.005$.

SUPPLEMENTARY MATERIAL

Supplementary Material is available at HMG Online.

ACKNOWLEDGEMENTS

We thank J.W. Gray for critically reading the manuscript and Drs K.P. Lu and T. de Lange for providing the TRF1 and TRF2$^{\Delta B\Delta M}$ constructs. This work was supported by American Cancer Society Institutional Research Grant no. 97-150-01-IRG, an Avon Foundation Gift, NIH Grant R21 CA87522-01, UC-BCRP Grant 6JB0133, NS42927, CA85799 and Brain Tumor SPORE P50 CA 97527. G.B.M. was supported by P50 CA83639, PO1 CA64602 and PO1 CA099031.

Conflict of Interest statement. The authors have declared that no conflict of interest exists.

REFERENCES

1. Kallioniemi, A., Kallioniemi, O.-P., Piper, J., Tanner, M., Stokke, T., Chen, L., Smith, H.S., Pinkel, D., Gray, J.W. and Waldman, F.M. (1994) Detection and mapping of amplified DNA sequences in breast cancer by comparative genomic hybridization. *Proc. Natl Acad. Sci. USA*, **91**, 2156–2160.
2. Werner, M., Mattis, A., Aubele, M., Cummings, M., Zitzelsberger, H., Hutzler, P. and Hofler, H. (1999) 20q13.2 amplification in intraductal

hyperplasia adjacent to *in situ* and invasive ductal carcinoma of the breast. *Virchows Arch.*, **435**, 469–472.
3. Tanner, M., Tirkkonen, M., Kallioniemi, A., Holli, K., Collins, C., Kowbel, D., Gray, J.W., Kallioniemi, O.-P. and Isola, J. (1995) Amplification of chromosomal region 20q13 in invasive breast cancer: prognostic implications. *Clin. Cancer Res.*, **1**, 1455–1461.
4. Collins, C., Volik, S., Kowbel, D., Ginzinger, D., Ylstra, B., Cloutier, T., Hawkins, T., Predki, P., Martin, C., Wernick, M. *et al*. (2001) Comprehensive genome sequence analysis of a breast cancer amplicon. *Genome Res.*, **11**, 1034–1042.
5. Schrock, E., Thiel, G., Lozanova, T., du Manoir, S., Meffert, M.C., Jauch, A., Speicher, M.R., Nurnberg, P., Vogel, S. and Janisch, W. (1994) Comparative genomic hybridization of human malignant gliomas reveals multiple amplification sites and nonrandom chromosomal gains and losses. *Am. J. Pathol.*, **144**, 1203–1218.
6. Ried, T., Knutzen, R., Steinbeck, R., Blegen, H., Schrock, E., Heselmeyer, K., du Manoir, S. and Auer, G. (1996) Comparative genomic hybridization reveals a specific pattern of chromosomal gains and losses during the genesis of colorectal tumors. *Genes Chromosomes Cancer*, **15**, 234–245.
7. Muleris, M., Almeida, A., Gerbault-Seureau, M., Malfoy, B. and Dutrillaux, B. (1994) Detection of DNA amplification in 17 primary breast carcinomas with homogeneously staining regions by a modified comparative genomic hybridization technique. *Genes Chromosomes Cancer*, **10**, 160–170.
8. Schlegel, J., Stumm, G., Scherthan, H., Bocker, T., Zirngibl, H., Ruschoff, J. and Hofstadter, F. (1995) Comparative genomic *in situ* hybridization of colon carcinomas with replication error. *Cancer Res.*, **55**, 6002–6005.
9. Iwabuchi, H., Sakamoto, M., Sakunaga, H., Ma, Y.Y., Carcangiu, M.L., Pinkel, D., Yang-Feng, T.L. and Gray, J.W. (1995) Genetic analysis of benign, low-grade, and high-grade ovarian tumors. *Cancer Res.*, **55**, 6172–6180.
10. Collins, C., Rommens, J.M., Kowbel, D., Godfrey, T., Tanner, M., Hwang, S., Polikoff, D., Nonet, G., Cochran, J., Myambo, K. *et al*. (1998) Positional cloning of ZNF217 and NABC1: genes amplified at 20q13.2 and overexpressed in breast carcinoma. *Proc. Natl Acad. Sci. USA*, **95**, 8703–8708.
11. Pieler, T. and Bellefroid, E. (1994) Perspectives on zinc finger protein function and evolution—an update. *Mol. Biol. Rep.*, **20**, 1–8.
12. Iuchi, S. (2001) Three classes of C2H2 zinc finger proteins. *Cell. Mol. Life Sci.*, **58**, 625–635.
13. Laity, J.H., Lee, B.M. and Wright, P.E. (2001) Zinc finger proteins: new insights into structural and functional diversity. *Curr. Opin. Struct. Biol.*, **11**, 39–46.
14. Comijn, J., Berx, G., Vermassen, P., Verschueren, K., van Grunsven, L., Bruyneel, E., Mareel, M., Huylebroeck, D. and van Roy, F. (2001) The two-handed E box binding zinc finger protein SIP1 downregulates E-cadherin and induces invasion. *Mol. Cell*, **7**, 1267–1278.
15. You, A., Tong, J.K., Grozinger, C.M. and Schreiber, S.L. (2001) CoREST is an integral component of the CoREST-human histone deacetylase complex. *Proc. Natl Acad. Sci. USA*, **98**, 1454–1458.
16. Shi, Y., Sawada, J., Sui, G., Affar el, B., Whetstine, J.R., Lan, F., Ogawa, H., Luke, M.P. and Nakatani, Y. (2003) Coordinated histone modifications mediated by a CtBP co-repressor complex. *Nature*, **422**, 735–738.
17. Grooteclaes, M., Deveraux, Q., Hildebrand, J., Zhang, Q., Goodman, R.H. and Frisch, S.M. (2003) C-terminal-binding protein corepresses epithelial and proapoptotic gene expression programs. *Proc. Natl Acad. Sci. USA*, **100**, 4568–4573.
18. Savelieva, E., Belair, C.D., Newton, M.A., DeVries, S., Gray, J.W., Waldman, F. and Reznikoff, C.A. (1997) 20q gain associates with immmortalization: 20q13.2 amplification correlates with genome instability in human papillomavirus 16 E7 transformed human uroepithelial cells. *Oncogene*, **14**, 551–560.
19. Doroshow, J.H. (1996) *Cancer Chemotherapy and Biotherapy*. Lippincott-Raven, Philadelphia.
20. Nonet, G., Stampfer, M.R., Chin, K., Gray, J.W., Collins, C.C. and Yaswen, P. (2001) The *ZNF217* gene amplified in breast cancers promotes immortalization of human mammary epithelial cells. *Cancer Res.*, **61**, 1250–1254.
21. Karlseder, J., Broccoli, D., Dai, Y., Hardy, S. and de Lange, T. (1999) p53- and ATM-dependent apoptosis induced by telomeres lacking TRF2. *Science*, **283**, 1321–1325.
22. Kishi, S., Wulf, G., Nakamura, M. and Lu, K.P. (2001) Telomeric protein Pin2/TRF1 induces mitotic entry and apoptosis in cells with short telomeres and is down-regulated in human breast tumors. *Oncogene*, **20**, 1497–1508.
23. Nicholson, K. and Anderson, NG. (2002) The protein kinase B/Akt signalling pathway in human malignancy. *Cell. Signal.*, **14**, 381–395.
24. Hanada, M., Feng, J. and Hemmings, BA. (2004) Structure, regulation and function of PKB/AKT—a major therapeutic target. *Biochim. Biophys. Acta*, **1697**, 3–16.
25. Courjal, F., Cuny, M., Rodriguez, C., Louason, G., Speiser, P., Katsaros, D., Tanner, M.M., Zeillinger, R. and Theillet, C. (1996) DNA amplifications at 20q13 and MDM2 define distinct subsets of evolved breast and ovarian tumours. *Br. J. Cancer*, **74**, 1984–1989.
26. Fang, X., Yu, S., LaPushin R., Lu, Y., Furui, T., Penn, L.Z., Stokoe, D., Erickson, J.R., Bast, R.C., Jr and Mills, G.B. (2000) Lysophosphatidic acid prevents apoptosis in fibroblasts via Gi-protein-mediated activation of mitogen-activated protein kinase. *Biochem. J.*, **352**, 135–143.